WCPFC–SC1 **ME WP–2**

1st Meeting of the Scientific Committee of the Western and Central Pacific Fisheries Commission
WCPFC–SC1
Noumea, New Caledonia
8–19 August 2005

Seapodym on a mixed-resolution spatial scale

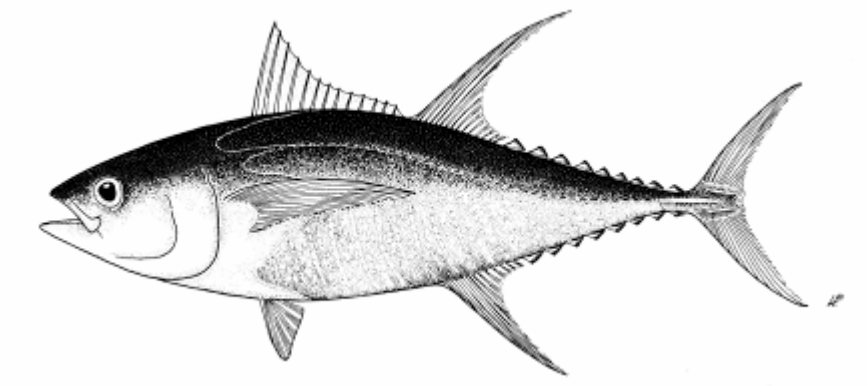

Senina, I.N., Sibert, J.R. and P. Lehodey

Pelagic Fisheries Research Programme, Honolulu, Hawaii.
Oceanic Fisheries Programme, Secretariat of the Pacific Community,
Noumea, New Caledonia

July 2005

Seapodym on a mixed-resolution spatial scale

[1]Inna N. Senina, [1]John R. Sibert, [2]P. Lehodey, [3]R. Murtugudde
[1]Pelagic Fisheries Research Program,
Joint Institute for Marine and Atmospheric Research
University of Hawai'i at Manoa, Honolulu, HI 96822, U.S.A.
[2]Secretariat of the Pacific Community,
Noumea, New Caledonia.
[3]Earth System Science Interdisciplinary Center,
University of Maryland, College Park, MD 20742, U.S.A.

July 29, 2005

Abstract

A spatial ecosystem and population dynamics model (SEAPODYM) for simulating spatial structure of tuna species based on advection-diffusion-reaction equations was implemented with mixed-resolution grid. Non-regularity of the grid is circumscribed by analytical stretching functions, which allow generation of grid node concentrations in particular regions and enhance the accuracy of the algorithm used to numerically solve PDE's. Transformation to orthogonal or non-orthogonal grids is taken into account in the numerical scheme by derivatives of the stretching functions as a grid metrics. With this approach, the number of nodes as well as the cost for numerical computations remain the same as for the model working on uniform grid. A computer tool for grid generation was developed. It allows building of land masks for arbitrary depth and transfer data utilized by the model onto designed grids. Numerical simulations were performed to test how finer grid resolution in areas of large variations in environmental data or fish biomass can improve the results of simulations for population of skipjack. Two mixed-resolution grids were created - with higher resolution in Kuroshio extension region (35N,130E,25S,160E) and WCPO area (20N,120E,20S,180E).

1 Introduction

Establishing the reasonably fine spatial resolution in the numerically solved partial differential equations (PDEs) is necessary for numerical solution to have the properties of corresponding analytical system. In the other words, the grid resolution should be sufficient to capture the scale of phenomena described by the model. Of course, simply increasing the number of nodes gives more accurate approximation of PDE, however for large domains, such as Pacific ocean, it significantly increases the computational load. Introducing the mixed-resolution grid can solve both problems by increasing the number of nodes only where it is necessary and thus avoiding extensive calculations. With this technique, the regions with finer resolution can be chosen dynamically following some criterion (adaptive grids) or defined statically during computational cycle if there exist permanent problematic areas such as currents convergence zones, complex boundaries or regions with sharp gradients.

There are several methods of mixed-resolution grid generation. Among them the most widespread for solving finite difference approximations of PDE are multi-grid approach, see e.g. Wesseling (1992), involving building of composite or nested grids and stretching approach (Liseikin, 1999), which consists of transformation of grid coordinates with help of algebraic techniques. The advantage of multi-grid approach is its efficacy in solving the system having components with different scales of variation. The stretching method consists in using analytical functions for grid transformation which makes grid generation fast and allows control of grid spacing by stretching functions parameters. Also, grid stretching doesn't change the number of nodes and doesn't increase the number of iterations while method of nested grid requires at least two iterations because solution on the coarse grid serves as an approximation for computation on the finer grid, which in turn corrects approximation error.

Another motivation for having variable resolution is availability of fine-resolution data in some regions, such as fishery catch and effort records, predicted or observed environmental data. So, we can define the appropriate resolution only in specific zones while keeping reasonable grid on the rest of the domain. Seapodym uses large amount of environmental and fisheries data, which should be interpolated on variable grid nodes. It makes introduction of adaptive grids, which change resolution depending on appearance of singularities during the simulations, not appropriate. Thus, Seapodym was implemented with the tool for generation of static non-uniform grids.

This paper is devoted to the detailed description of Seapodym and to the application of the stretching grids approach to this model.

2 Model

Seapodym is a two-dimensional spatio-temporal model describing tuna and its forage population distributions with help of advection-diffusion-reaction equations with chemotaxis (movement in response to a habitat gradient) for actively migrating adult individuals (see, e.g. Okubo, 1980). The state variables represent components of predator-prey system: 6 populations of tuna forage classified by vertical layers where they inhabit (epipelagic, mesopelagic and bathypelagic); and age-structured predator population (tunas). Seapodym can be parameterized as a multi-species model, but in this paper it is described as single-species one. Model estimates of primary production, temperature and oceanic currents in three depth layers (provided by the Earth System Science Interdisciplinary Center of the University of Maryland) and dissolved oxygen climatological fields (from Levitus database) are Seapodym inputs. All spatio-temporal processes in tuna population such as migrations, spawning, recruitment, survival and mortality are circumscribed by conditions of physical environment. The detailed mathematical description of the model is given in Appendix A. Seapodym predicts biomasses of forage populations and tuna age classes, catches by different fisheries, computes spatial correlations between predicted and observed catch data and length frequencies in the catch by fishery.

3 Methods

Let $(x, y) = (i\Delta x, j\Delta y)$ be the coordinates of regular grid and (ξ, ζ) the coordinates of mixed-resolution grid. Stretching function $f(x) : x \rightarrow \xi$ performs transformation of the regular domain coordinates to stretched ones, correspondingly the inverse function $f^{-1}(\xi)$ returns coordinates to the regular positions. The finite difference approximation of the PDE's is performed on the regularly spaced grid. In order to compute the solution of PDE on the variable grid, one should convert it to the uniform grid and use the same numerical scheme for this logical domain taking into account analytical metrics defining grid transformation. Since we will generate the mixed-resolution grid just once we actually do not need to know the stretching functions itself but the inverse functions, which transforms the desired variable grid to regular coordinate system (x, y). The coordinates of stretched grid can be found numerically by solving nonlinear equation $f^{-1}(\xi) - x = 0$.

The stretching function can be one-dimensional, i.e. providing transformation of the grid coordinates along one direction through the whole domain, or two-dimensional, which allows us to transform grid coordinates locally and create curvilinear coordinates. Thus, two types

of stretching functions are applied to transform regular grid to the non-uniform one:

$$x_i = f^{-1}(\xi_i) \qquad x_{ij} = \phi^{-1}(\xi_i, \zeta_j)$$
$$y_j = g^{-1}(\zeta_j) \qquad y_{ij} = \psi^{-1}(\xi_i, \zeta_j)$$

Also, the composition of these two functions can be used to obtain grid point concentrations around specified centers combining one-dimensional with local non-orthogonal stretching.

The first type of function is based on multi-mode arctan function:

$$x_i = a + b\left(\xi_i + \sum_{k=1}^{N} \alpha_k \arctan(\beta_k^{-1}(\xi_i - \gamma_k)\right) + c{\xi_i}^2, \tag{1}$$

where positive parameters α_k increase resolution in the vicinity of points γ_k, coefficients β_k respond for the width of the area where the grid has higher resolution (or the opposite in case of negative α_k). The same transformation can be applied to the y axes. Parameters a and b should be found in order to confirm the boundaries, i.e. by solving algebraic system of two equations to provide $x_0 = \xi_0$, $x_n = \xi_n$. Nonzero parameter c is used to fix chosen grid coordinate inside domain $x_i = \xi_i$. This can be useful if we need to move grid nodes only on one side from this point and keep other points static.

The function for two-dimensional stretching is Gaussian:

$$x_{ij} = \xi_{ij} + \sum_{k=1}^{N} \delta_{\xi k}(\xi_{ij} - \bar{\xi}_k) e^{-\left(\frac{\xi_{ij}-\bar{\xi}_k}{\sigma_{\xi k}}\right)^2 - \left(\frac{\zeta_{ij}-\bar{\zeta}_k}{\sigma_{\zeta k}}\right)^2}, \tag{2}$$

$$y_{ij} = \zeta_{ij} + \sum_{k=1}^{N} \delta_{\zeta k}(\zeta_{ij} - \bar{\zeta}_k) e^{-\left(\frac{\xi_{ij}-\bar{\xi}_k}{\sigma_{\xi k}}\right)^2 - \left(\frac{\zeta_{ij}-\bar{\zeta}_k}{\sigma_{\zeta k}}\right)^2}, \tag{3}$$

where $(\bar{\xi}_k, \bar{\zeta}_k)$ are the central points of N transformed areas, coefficients $\delta_{\xi k}$ and $\delta_{\zeta k}$ define the skewness of the grid, the sign of these coefficients determine whether grid will be stretched or concentrated around center. Coefficients $\sigma_{\xi k}$ and $\sigma_{\zeta k}$ give the width of the area where the grid will be transformed. As it is seen from the formulas (1) and (2,3), the multiple high-resolution areas can be generated.

Note, that two-coordinate functions (2,3) are not boundary conforming, i.e. conditions $x_{0j} = \xi_{0j}$, $y_{i0} = \zeta_{i0}$ are not satisfied. So, increasing δ and σ coefficients, one should be careful to avoid acting on the bounds, except the case of moving only those grid nodes, which belong to the land mask.

The changes in numerical scheme due to introducing mixed resolution are minor. The derivatives of function (1) and (2,3) serves as a new grid metrics and partial derivatives in PDE over non-uniformly spaced coordinates ξ can be represented as

$$\frac{\partial}{\partial \xi} = \frac{\partial}{\partial x} \cdot \frac{dx}{d\xi} \tag{4}$$

Hence finite difference approximations remain the same and in order to use the numerical scheme on a regularly spaced grid we only need to know the metrics $\frac{dx}{d\xi}$ of variable resolution.

Although the principle of introducing the stretched grids is extremely simple, it requires a lot of extra operations for the whole model to be properly set on mixed-resolution. First of all, grid stretching leads to the task of building new land mask. For this purpose the software Grid and Mask Builder (GMB) was created and further developed as a 'plugin' for Seapodym, which accomplishes all necessary work on variable grid. Using ETOPO2 (2-minute gridded global relief data, see information on http://www.ngdc.noaa.gov/mgg/global) topography maps in GMB made it possible to create multi-level land masks for arbitrary chosen depth layers. For transferring input environmental data such as ocean currents, temperature, oxygen and primary production onto new grids, GMB includes a cubic splines interpolation routine and for interpolating sparse catch data averaged over 1° or 5° square cells there is the routine for redistributing data onto generated grid with help of weigths being new cell's areas.

4 Results

First, the conservative properties of the numerical solution of equations (A1-A3) with zero mortality were verified on both types of stretched grids. Then simulations with complete dynamics model described in Appendix A were performed. Two areas that play an important role for skipjack biology, namely Western-Central Pacific ocean (20N,120E,20S,180E) being the major region of skipjack recruitment and Kuroshio extension region (35N,130E,25S,160E), whose warm-core rings form excellent skipjack fishing ground (Lehodey *et al*, 2003) were chosen for experiments with mixed-resolution grid. The goal was to create finer resolution in the region where skipjack population is abundant while making reasonably coarse grid at the rest of the domain and to insure that simulations on non-uniform grid do not create a pronounced difference in predicted spatial distributions in comparison to modeling on regular grid and possibly allow us to get better fit of observed catch data due to more accurate numerical resolution of population dynamics in covered by fine resolution areas.

Three simulations were accomplished - one on a regular 1° square grid and two on mixed-resolution grids. The first non-uniform grid is orthogonal (see Fig. 1), generated with stretching function (1) in both horizontal directions. It covers WCPO region by 0.5° resolution and

approaches 4° in north-eastern and south-eastern Pacific (Fig. 2). Second, non-orthogonal grid was generated by composition of functions (1) and (2,3). It has 0.5° resolution locally in Kuroshio extension region, approximately 0.85° cell size along x and y axes with the center of intersection in Kuroshio and the maximal size of grid cells in the whole domain being 1.4°.

The results of simulations on mixed resolution grids with the same model parameterization are generally similar to results obtained by the model on regular grid. Figure 3 presents the dynamics of building skipjack population and further temporal development of aggregated over whole domain biomasses of juveniles (J_1 and J_2, see Appendix A), immature tuna (N_0 and N_1) and adults (sum of ages after 9 months old). Lower biomasses were obtained in 'WCPO' and 'Kuroshio' simulations than in regular grid simulations. Figure 4 shows the comparison of spatial distributions of juvenile and adult skipjack is shown. The spatial structures of juveniles have the same shape and localization, the biomass of adult skipjack seem to be more dispersed to the eastern Pacific in comparison to regular grid simulation.

The spatial correlations between predicted and observed catches of the fisheries operated mostly in western Pacific (Fig. 5) are higher in simulations on stretched grids. As was concluded by Lehodey *et al* (2003) finer resolution in Kuroshio region should improve the quality of model prediction for Japan domestic pole and line catch data and the experiment with 'Kuroshio' grid confirms it (see Fig. 6 and Table 1). However, predictions in ECPO look better in simulation on regular grid (see, e.g., spatial correlations in Table 1), which means that too coarse resolution was taken in this region. Obviously, a trade-off exists between concentrating grid nodes in some areas while reducing resolution elsewhere.

Additionally, the constructing of proper age structure in simulations on mixed-resolution grids is seen on the graphs with predicted and observed length frequencies in catches (Fig. 7). Both length frequences predicted with regular grid simulation and mixed-resolution one agree well with observations.

5 Conclusions

The experiments on mixed-resolution grid showed the feasibility of the stretched grid approach in Seapodym and good fit of predicted to observed catch data. GMB software allows generating non-uniform grids and transfering all necessary input data to variable resolution. Availability of fine-resolution fisheries data in the future is an opportunity to further evaluate the efficiency of the model on mixed-resolution scale.

The spatial and temporal dynamics of tuna population in Seapodym is stipulated by habitat indices, which in turn are linked to physical environment. Thus, proper determination of habitat indices values plays the crucial role in obtaining true qualitative and quantitative prediction of tuna population abundance and its spatial distribution. For this purpose the

method of adjoint model construction has been chosen as the most powerful tool for obtaining partial derivatives of objective function with respect to calibrating parameters (see, e.g., Griewank and Corliss, 1991). The same technique was earlier successfully implemented for the estimation of skipjack movement parameters from tagging data in advection-diffusion-reaction model (Sibert *et al*, 1999). The parameter estimation procedure is now accomplished for the sub-model without adult tuna, i.e. for system (A1-A2). Completing this task for the whole model is a very important step in further development of Seapodym and efficient use of mixed-resolution approach.

References

Bertignac, M., Lehodey, P. and J. Hampton. 1998. A spatial population dynamics simulation model of tropical tunas using a habitat index based on environmental parameters. *Fish. Oceanogr.* 7: 3/4, 326-334.

Griewank, A. and G.F. Corliss. 1991. Automatic differentiation of algorithms: theory, practice and application. SIAM, Philadelphia.

Lehodey, P, Chai, F. and J. Hampton. 2003. Modelling climate-related variability of tuna populations from a coupled ocean biogeochemical-populations dynamics model. *Fish. Oceanogr.* 12: 4/5, 483-494.

Lehodey, P. 2001. The pelagic ecosystem of the tropical Pacific Ocean: dynamic spatial modeling and biological consequences of ENSO. *Progress in Oceanography.* 49, 439-468.

Liseikin, V.D. 1999. Grid Generation Methods. Springer-Verlag, Heidelberg.

Okubo A. 1980. Diffusion and ecological problems: mathematical models. Springer-Verlag, NY.

Sibert, J.R., Hampton, J., Fournier, D.A. and P.J. Bills. 1999. An advection-diffusion-reaction model for the estimation of fish movement parameters from tagging data, with application to skipjack tuna (*Katsuwonus pelamis*). *Can. J. Fish. Aquat. Sci.* 56, 925-938.

Wesseling, P. 1992. An Introduction to Multigrid Methods. Chilchester.

Appendix A. Mathematical description of Seapodym

Spatio-temporal dynamics model Seapodym is based on advection-diffusion-reaction (ADR) continuous equations, which describe random and directed movements of tuna and forage populations and variation of population densities in time. In order to find the numerical solution of ADREs, they are discretized on a spatial grid and in time. At each discrete time step, the change of biomasses due to ageing, survival and reproduction are described by algebraic equations. Environmental factors are used to compute habitat indices, which constrain movement and demographic processes (Bertignac *et al*, 1998). Generally, the model can be split into two sub-models: forage recruitment sub-model and predator-prey (tuna-forage) sub-model with age-structured tuna population and mature forage populations.

The dynamics of tuna and forage populations is governed by the following environmental data: $\mathbf{v}_z$ is the vector of oceanic horizontal currents at depth layer z, T_z is the temperature at layer z, O_z is dissolved oxygen averaged through each layer and P is the primary production averaged through layer 0-400m. Currently three depth layers with thresholds 100m, 400m and 1000m are taken into account.

The model is two-dimensional, spatial coordinates (x, y) are the points of Pacific ocean domain $\Omega = \{x \in (90E, 68W), y \in (65N, 55S)\}$. Each state variable as well as variables of environment are determined at point (x, y) and time t (here and after we will omit the notations of space and time). Also, for shorter mathematical expressions for the derivatives of functions of two spatial variables we will use gradient operator $\nabla = (\frac{\partial}{\partial x}, \frac{\partial}{\partial y})$.

Forage recruitment model. Several forage populations differentiated by their habitat in depth are considered. Each population is split into two age groups by the time of maturity, when it becomes the food source for tuna. Let variables S_n, $n = 1..n_{max}$ (currently $n_{max} = 6$) denote the densities of the immature forage populations and F_n are the densities of mature forages. The age at which forage becomes mature, in the other words, the duration of recruitment is spatially dependent variable since we have to take into account regions as different as the warm pool and subarctic gyre (Lehodey *et al*, 2003). Thus, the time passed between spawning and maturing is linked to ambient temperature $\tau_n = \tau_n(T(x, y))$. Assuming that at higher temperature the younger organisms become mature, this dependence is $\tau_n = \tau_{max} e^{\alpha \hat{T}_n}$ with $\tau_{max} = 15(months)$ and negative slope coefficient α, determining non-linear decrease of recruits age with temperature $\hat{T}_n$ (symbol 'hat' denotes averaging over depth layers where forage populations inhabit during the day and night). This hypothesis is based on the well-known positive correlation between metabolic rate of organisms and ambient temperature. Since during the time τ_n immature forage population S_n is migrating, advection-diffusion equations with passive drift by oceanic currents are used to describe its spatial dynamics. Zero-flux boundary conditions are used to set impermeability of the domain and initial conditions $S_n^0 = cE_nP^0$, determine spawning in forage populations, where coefficients E_n are the

energy transfer constants, c is the forage specific value of unit conversion and P^0 is primary production biomass available at the time of population's spawning.

Thus, the recruits for mature forage population F_n at each time t, are defined by expression $R_n = S_n^m$, where time index $m = \lfloor \tau_n \rfloor$, i.e. due to spatially dependent τ_n the variable R_n incorporates the different spatial compartments (depending on the local temperature) of the solutions $S_n^0, S_n^1, .., S_n^{\tau_{max}}$ obtained by integrating numerically advection-diffusion equations for different time periods.

Tuna-forage coupled model. The state vector consists of the following variables: densities of mature forage populations F_n, densities of tuna larvae J_0, densities of juvenile monthly based age classes J_k, $k = 1, .., k_{max}$; and densities of adult quarterly based age classes N_a, $a = 1, .., a_{max}$. Population of skipjack is structurized into $k_{max} = 2$ juvenile classes and $a_{max} = 15$ adult age classes.

The system of advection-diffusion-reaction and chemotaxis equations describing transport of tuna and forage populations is:

$$\frac{\partial F_n}{\partial t} = -\hat{\mathbf{v}}\nabla F_n + \nabla(D\nabla F_n) - (\lambda_n + \omega_n) \cdot F_n + R_n \tag{A1}$$

$$\frac{\partial J_k}{\partial t} = -\mathbf{v}_0\nabla J_k + \nabla(D\nabla J_k) - g_k(P, F, T_0, N) \cdot J_k + R_k \tag{A2}$$

$$\frac{\partial N_a}{\partial t} = -\tilde{\mathbf{v}}\nabla N_a + \nabla(\sigma\nabla N_a - (\chi\nabla I_a, N_a)) - f_a(P, F, T, O) \cdot N_a + R_a \tag{A3}$$

where terms R_n, R_k and R_a represent the source of density for corresponding population or age group due to spawning, recruiting or ageing processes, λ_n, ω_n, g_k, f_a are mortality functions, parameter D is constant diffusion coefficient for forage populations, tuna larvae and juveniles, $\hat{\mathbf{v}}$ denotes oceanic currents averaged through the layers where forage presents at day and night time, I_a is the feeding habitat index, σ is the diffusion coefficient for adult tuna, determined by the habitat index value and its gradient:

$$\sigma = \sigma_{max}\left(1 - \frac{I_a}{\gamma + I_a}\right)(1 - \rho\nabla I_a) \tag{A4}$$

and $\chi = (\chi_x, \chi_y)$ is the coefficient of chemotactic movement toward the gradient of the habitat index I_a. Coefficients σ_{max} and χ are proportional to maximum sustainable speed of the fish. Parameters γ and ρ are chosen to balance diffusive and advective movement on the hypothesis that maximal displacement due to both diffusion and taxis do not exceed the distance which fish can swim with its maximal sustainable speed per unit of time.

The system is completed by Neuman boundary conditions describing impermeability of the ocean domain bounds $\partial\Omega$:

$$\mathbf{n} \cdot \mathbf{v}\Big|_{\mathbf{x}\in\partial\Omega} = \mathbf{n} \cdot \nabla F_n\Big|_{\mathbf{x}\in\partial\Omega} = \mathbf{n} \cdot \nabla J_k\Big|_{\mathbf{x}\in\partial\Omega} = \mathbf{n} \cdot \nabla N_a\Big|_{\mathbf{x}\in\partial\Omega} = 0 \tag{A5}$$

These conditions mean no additional source of biomass and no loss when recruitment and mortality are absent. Initial conditions are zero densities of tuna population age classes and non-zero densities of forage recruits.

Thus, in the system (A1-A3) we have $n_{max} + 1 + k_{max}$ advection-diffusion-reaction equations plus a_{max} equations with taxis for adults and $n_{max} \times \tau_{max}$ advection-diffusion equations in forage recruitment sub-model solved at each time step. The partial derivatives of ADEs are approximated by second order finite differences with upwind differencing of advective terms. The resulting algebraic problem is solved with help of alternate direction implicit (ADI) method. Since sub-model for S_n components is totally independent from forage-tuna system variables, the distributions of forage recruits can be build separately, which simplifies the numerical resolution of the entire model.

Three types of habitat indices determine response of tuna on physical environment conditions. These are feeding, spawning and juvenile's habitat index. The definition of these indices influence on spatial and temporal dynamics of tuna and consequently forage populations. All indices are scaled to be in interval $(0, 1)$.

Feeding habitat index I_a is the function of forage density, primary production, temperature and oxygen and has the following form:

$$I_a = r^{\delta \frac{dL}{dt}} \sum_n \Theta_n F_n \tag{A6}$$

where base r is the ratio of primary production to forage biomass in the habitat, δ is a constant and L is the day length L. $\Theta_n = \Phi_n(T)\Psi_n(O)$ is the accessibility function and the sum describes how much food is accessible to predator during light and dark time of the day. $\Phi_n(T)$ is a Gaussian function averaged over day time of each forage population, i.e.

$$\Phi_n(T) = \frac{c}{\sigma\sqrt{2\pi}} \left(L_l e^{-\left(\frac{T_{n_l} - T_{opt}}{2\sigma}\right)^2} + L_d e^{-\left(\frac{T_{n_d} - T_{opt}}{2\sigma}\right)^2} \right), \tag{A7}$$

$$T_{opt} = \frac{T_a - T_s}{a_{max}} a + T_s, \tag{A8}$$

$$\tag{A9}$$

where indices l and d denote light and dark part of the day, T_a is the mean temperature for age class a and T_s is the temperature at spawning. Thus, the link between the age of tuna and its response to the temperature in habitat index is established. Ψ_n is a sigmoid function of oxygen:

$$\Psi_n(O) = \left(1 + e^{\gamma(O - O_{cr})}\right)^{-1}. \tag{A10}$$

Spawning habitat index used to constrain the number of larvae is the function of SST, primary production and forage biomasses:

$$I_s = r^{\delta}\Phi(T_0), \text{ where } \Phi(T_0) = \frac{c}{\sigma_0\sqrt{2\pi}} e^{-\left(\frac{T_0 - T_{0_{opt}}}{2\sigma_0}\right)^2} \tag{A11}$$

where parameter δ is the same as in accessibility function described above and ratio r is the ratio of primary production to forage biomass on the surface during the day.

Juvenile habitat index is a function of tuna biomass as well as environmental factors used to compute the mortalities for juvenile age class:

$$I_j = ln(1 + \frac{P}{\sum_a (N_a)})\Phi(T_0), \tag{A12}$$

Tuna spawning is proportional to the spawning habitat value (A9):

$$J_0 = \kappa I_s \tag{A13}$$

with κ giving the maximal number of larvae in the habitat since $0 < I_s < 1$.

Tuna survivors of each age class are computed as a number of individuals remaining in the age class plus recruits from younger age and minus the number of individuals which pass to the older age group. Thus, we have simple relationships:

$$J_k = q_{k-1}J_{k-1} + (1 - q_k)J_k, k = 1, 2 \tag{A14}$$

$$N_0 = q_k J_2 + (1 - q_0)N_0, \tag{A15}$$

$$N_a = q_{a-1}N_{a-1} + (1 - q_a)N_a, \tag{A16}$$

where survival coefficients q_k and q_a determine the rates of decay of the density due to both natural and predation mortality depending on the time spent in corresponding age, they are values between 0 and 1, so that

$$q_a = \frac{1}{\sum\limits_{i=0}^{\xi-1} e^{-iM_a}} e^{-(\xi-1)M_a} \tag{A17}$$

Here ξ is characteristic time of corresponding age class being one month for juveniles and one quarter for adults for the population of skipjack (Lehodey, 2001).

Forage mortality Natural and predation mortalities of forage populations in equation (A1), λ_n and ω_n correspondingly, are determined as follows:

$$\lambda_n = \left(\lambda_{max} e^{\mu \hat{T_n}}\right)^{-1} \tag{A18}$$

$$\omega_n = \omega_{n_N} - \hat{\omega}_n \tag{A19}$$

Local mortality due to tuna predation ω_{n_N} is spatially dependent and total predation mortality $\hat{\omega}_n$ of each forage species is aggregated value over the whole domain:

$$\omega_{n_N} = \frac{1}{F_n}\left(\sum_a \left(N_a W_a G_a \frac{\Theta_n}{\sum_n \Theta F_n}\right)\right) \tag{A20}$$

$$\hat{\omega}_n = \frac{\sum\limits_{\Omega}(\omega_{n_N} F_n)}{\sum\limits_{\Omega} F_{n_{pred}}} \tag{A21}$$

Here W_a is the weight of tuna at age a and G_a is the daily food ration, $F_{n_{pred}}$ is the biomass of n-th forage population in the habitat where predators are presented and Θ_n is the accessibility function described above.

Tuna mortality functions g_k and f_a are similar to each other, including natural or senescence mortality M_s and predation mortality M_p, but depending on different habitat indexes defined for every age class - larvae habitat index I_{sp}, juvenile habitat index I_j and feeding habitat index for adult tuna I_a. Also, fishing mortality is taken into account for obtaining total mortality rate of adult age classes.

$$g_0 = (M_s + M_p)(1+\epsilon)^{1-2I_{sp}} \tag{A22}$$

$$g_k = (M_s + M_p)(1+\epsilon)^{1-2I_j}, k = 1,2 \tag{A23}$$

$$f_a = (M_s + M_p)(1+\epsilon)^{1-2I_a} + M_f, a = 1,..,15 \tag{A24}$$

where non-zero parameter ϵ assigns variability of species mortality with habitat index, senescence predation and fishing mortalities are described as follows:

$$M_s = M_{s_{max}}\left(1 + e^{\xi(a-\zeta)}\right)^{-1}, \tag{A25}$$

$$M_p = M_{p_{max}} e^{-\lambda a}, \tag{A26}$$

$$M_f = s_{ak} q_{ak} E_k. \tag{A27}$$

Observed efforts E_k are given for each fleet k. Coefficients s_{ak} and q_{ak} are the selectivity and catchability parameters correspondingly, which depending on fishing gears used by fleet.

Figure 1: One-dimensional grid stretching in WCPO region and three-layer mask generated by GMB. Land mask is build for 0-100m (grey rectangles), 100-400m (light grey) and deeper 400m (white) layers. The smallest grid resolution is 0.5°.

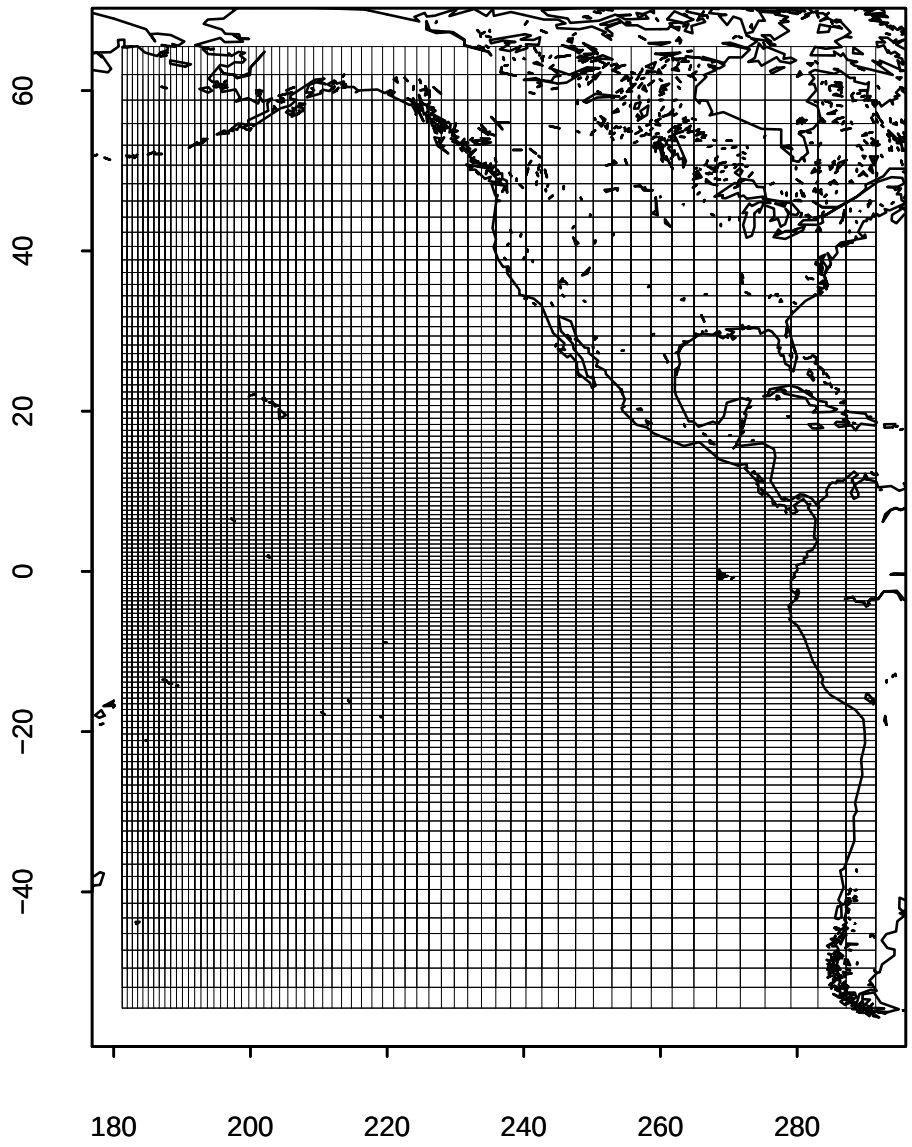

Figure 2: 'WCPO' grid in eastern Pacific. The largest resolution in longitude and lattitude is 4°.

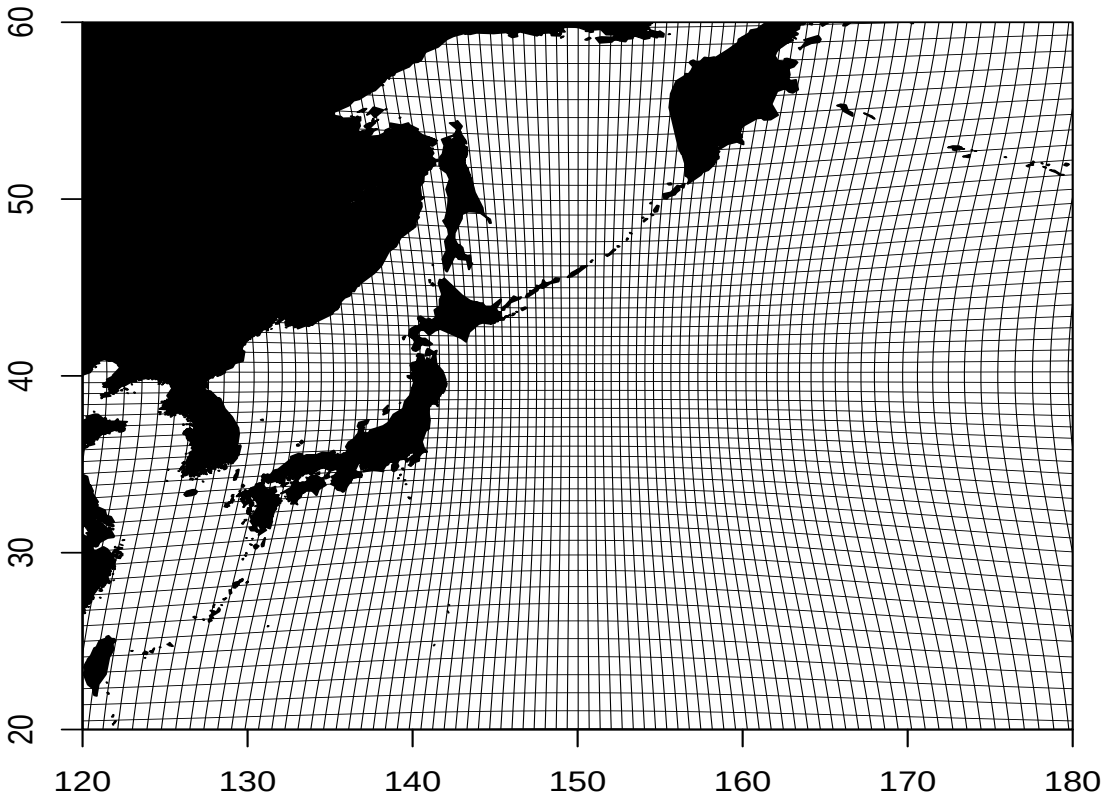

Figure 3: An example of combination of one-dimensional and two dimensional stretching applied to get 0.5° resolution in Kuroshio region. The total number of grid nodes covering Pacific ocean domain is 203×121 and the largest spacing is 1.4°.

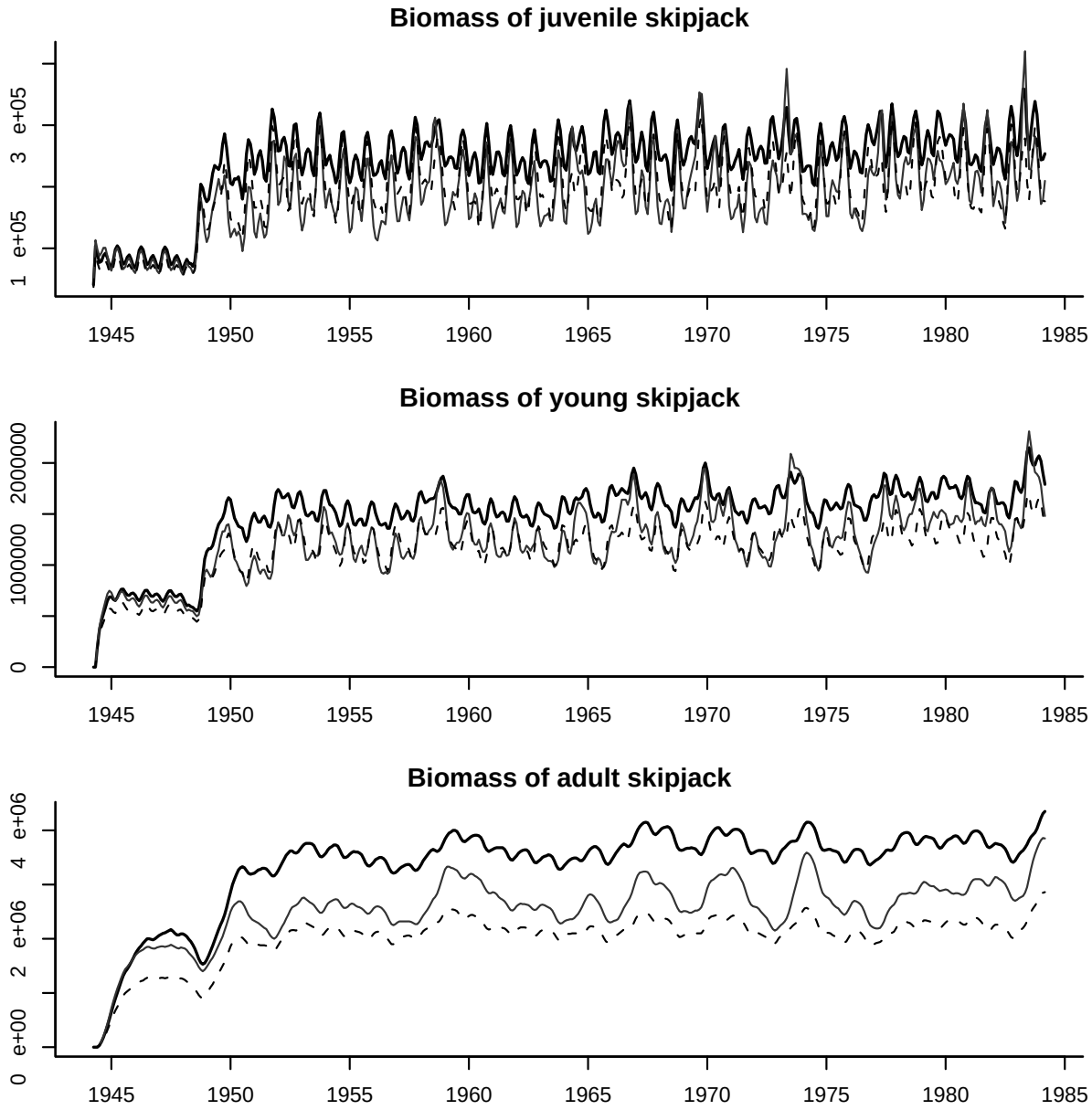

Figure 4: Build up and temporal dynamics of skipjack tuna population with two years of stock forecasting. Thick line shows results of simulation on regular grid, dashed line is obtained by 'WCPO' run and dotted line presents the aggregated dynamics in 'Kuroshio' simulation.

a) Juvenile skipjack, regular grid

b) Juveniles, mixed-resolution grid

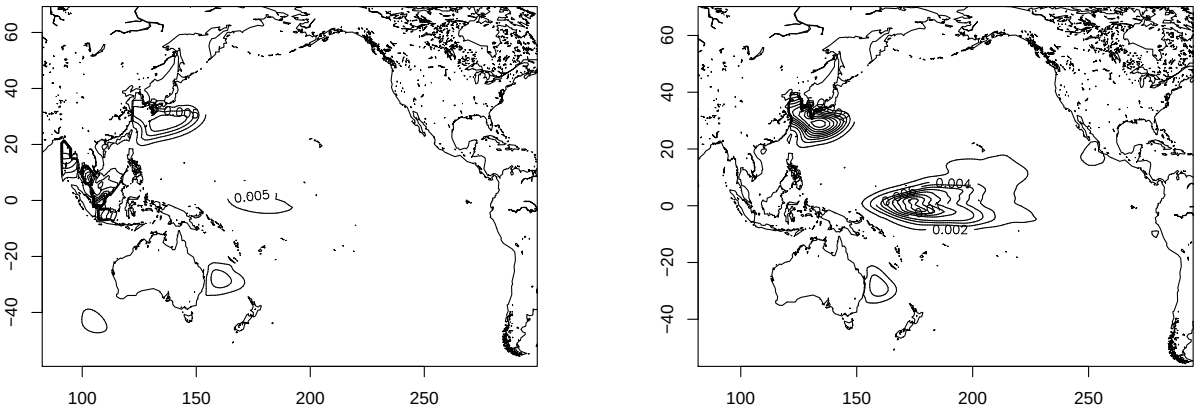

c) Adult skipjack, regular grid

b) Adults, mixed-resolution grid

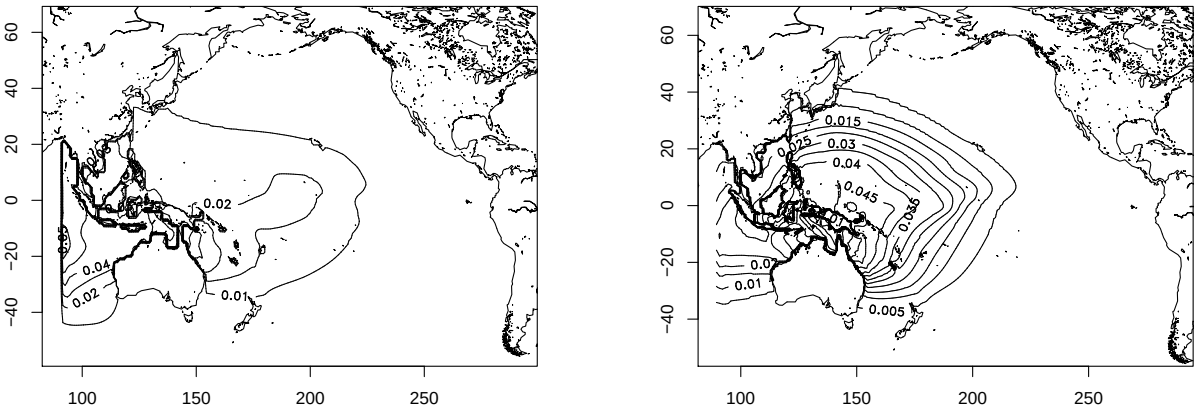

Figure 5: Spatial distribution of skipjack population predicted for July 1004 and represented by isopleths of biomass.

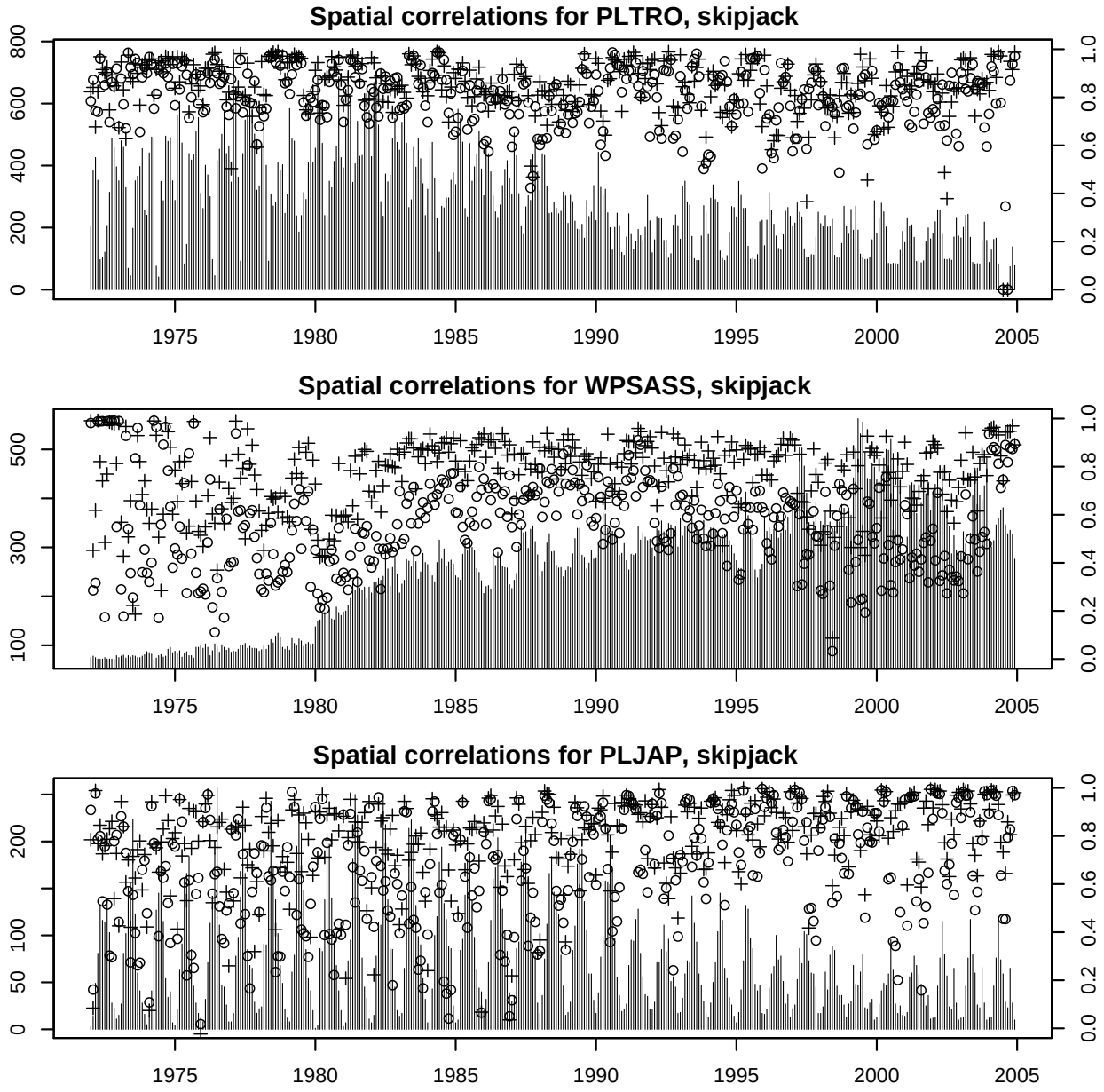

Figure 6: Comparison of spatial correlations between observed and predicted catch in simulation on regular grid (circles) and KUROSHIO grid (crosses). Observed catch data presented for Pole and Line Japan fleet, PL tropical fleet and Western Pacific 'associated' (log, fad, animals) fisheries.

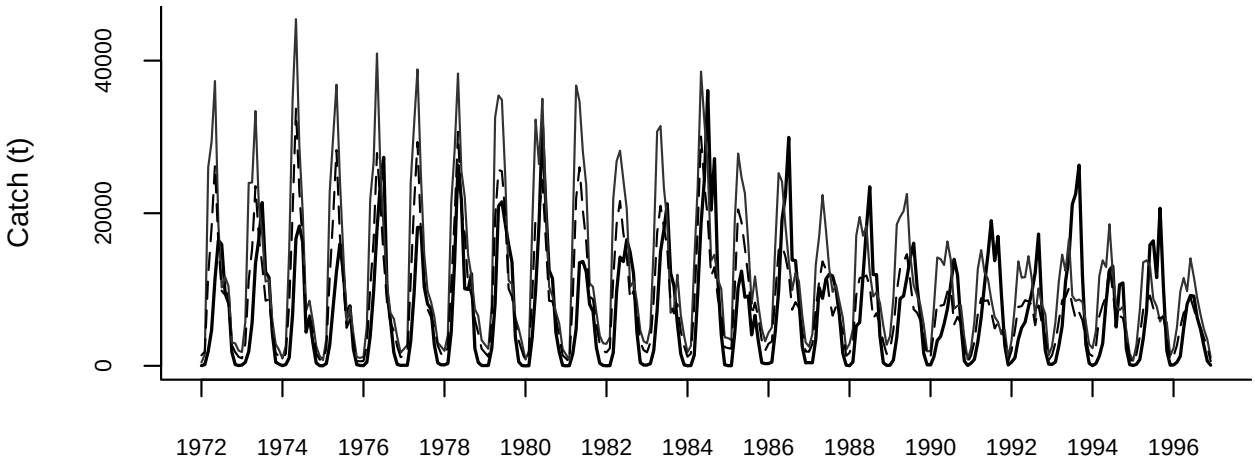

Figure 7: Comparison of observed (thick solid line) and predicted catches for Pole and Line Japan fleet (thin solid line denotes results of simulation on regular grid, dashed line - simulation on KUROSHIO grid).

Table 1: Averaged spatial correlations between observed catch data for fishery and predicted by simulations on regular and mixed-resolution grids. The extreme coordinates of data available for each fleet are also given.

N	Fishery	x_E	x_W	y_N	y_S	R_{reg}	R_{WCPO}	$R_{KUROSHIO}$
1	PL Japan	120.5	226.5	46.5	25.5	0.66	0.73	0.79
2	PL Tropical	110.5	228.5	24.5	-47.5	0.81	0.85	0.84
3	WPO PS associated	114.5	208.5	49.5	-51.5	0.58	0.68	0.77
4	WPO PS unassociated	114.5	208.5	46.5	-51.5	0.69	0.73	0.80
5	EPO PS associated	209.5	285.5	33.5	-24.5	0.63	0.55	0.50
6	EPO PS unassociated	209.5	282.5	36.5	-25.5	0.62	0.58	0.51

A

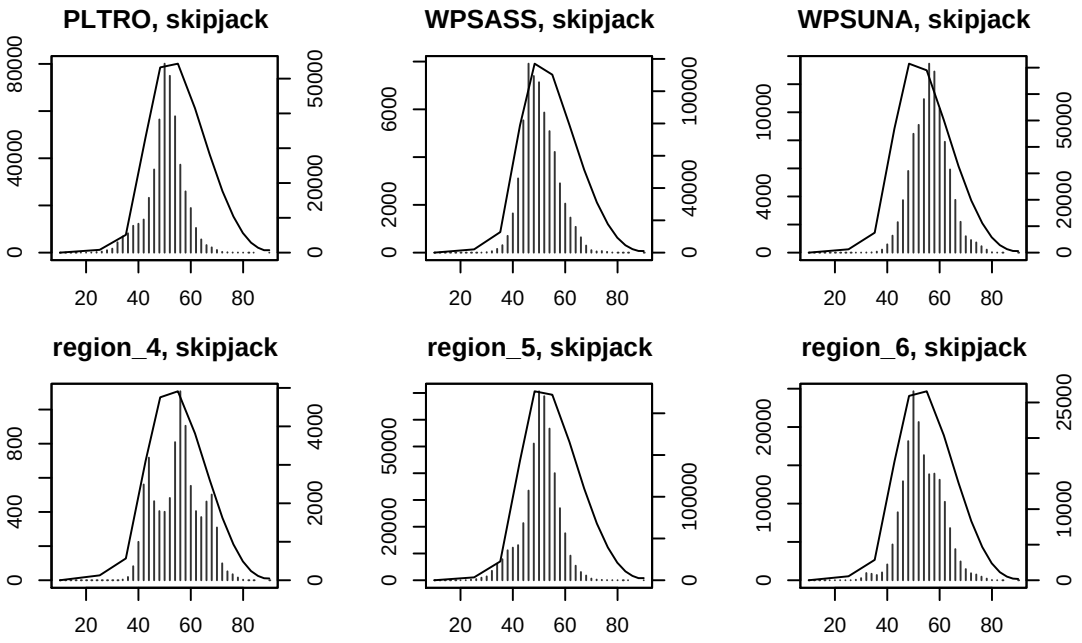

B

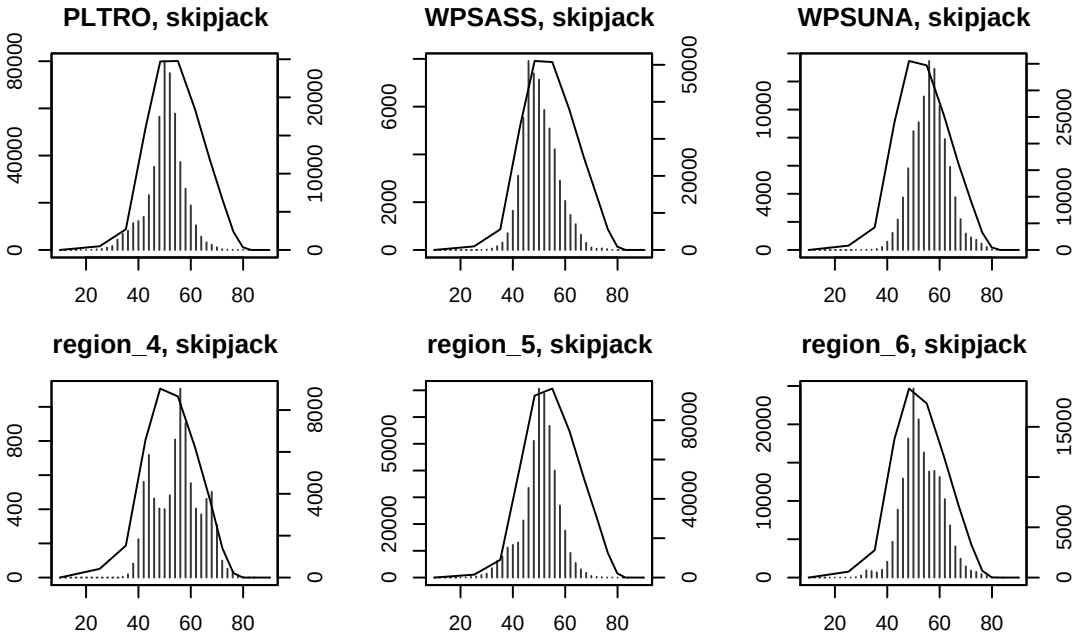

Figure 8: Predicted (lines) and observed (histogram) length frequences in the catch. Graphs A represents the results of simulations on regular grid, B - WCPO grid.